Synaptic Rewiring for Topographic Map Formation

Synaptic Rewiring for Topographic Map Formation

Simeon A. Bamford[1], Alan F. Murray[2], and David J. Willshaw[3]

[1] Doctoral Training Centre in Neuroinformatics, sim.bamford@ed.ac.uk,
[2] Institute of Integrated Micro and Nano Systems
[3] Institute of Adaptive and Neural Computation,
University of Edinburgh

Abstract. A model of topographic map development is presented which combines both weight plasticity and the formation and elimination of synapses as well as both activity-dependent and -independent processes. We statistically address the question of whether an activity-dependent process can refine a mapping created by an activity-independent process. A new method of evaluating the quality of topographic projections is presented which allows independent consideration of the development of a projection's preferred locations and variance. Synapse formation and elimination embed in the network topology changes in the weight distributions of synapses due to the activity-dependent learning rule used (spike-timing-dependent plasticity). In this model, variance of a projection can be reduced by an activity dependent mechanism with or without spatially correlated inputs, but the accuracy of preferred locations will not necessarily improve when synapses are formed based on distributions with on-average perfect topography.

1 Introduction

The development of topographic mappings in the connections between brain areas is a subject that continues to occupy neuroscientists. There have been a number of investigations of the development of maps through networks with fixed connectivity and changes to synaptic weights [1–5]. Other models have considered the formation and elimination of synapses with fixed weight [6]. Indeed a mathematical equivalence between such models has been demonstrated for certain conditions [7]. There have been few attempts to include both forms of plasticity in a model (though see [8, 9]) however since both forms of plasticity are known to exist, we have created a model of topographic map development which combines both forms of plasticity and we explore some of the consequences of this model. This work is part of an overall project to implement synaptic rewiring in neuromorphic VLSI [10], however the model and results presented here are purely computational.

Theories of topographic map formation can be divided by the extent to which activity-dependent processes, based on Hebbian reinforcement of the correlated

activity of neighbouring cells, are deemed responsible for the formation of topography. Some assume that activity-independent processes, based on chemoaffinity [11] provide an approximate mapping, which is then refined [12]. Others [5, 13] show how activity-independent processes may fully determine the basic topography, thus relegating the role of activity-dependent processes to the formation of "functional architecture" e.g. oculardominance stripes etc. [14]. Our model is in the latter of these categories, assuming that synapses are placed with on-average perfect topography by an activity-independent process. Miller [7] gives evidence that the decision whether newly sprouted synapses are stabilized or retracted may be guided by changes in their physiological strengths; this is a basis for our model.

2 Model

This generalised model of map formation could equally apply to retino-tectal, retino-geniculate or geniculo-cortical projections. There are 2 layers (i.e. 2D spaces on which neurons are located), the input layer and the network layer. Each location in one layer has a corresponding "ideal" location in the other, such that one layer maps smoothly and completely to the other. For simplicity neural areas are square grids of neurons and the 2 layers are the same size (16 x 16 in the simulations presented here). We have worked with small maps due to computational constraints; this has necessitated a rigorous statistical approach, which is an overdue development in this field, as noted by [14]. Periodic boundaries are imposed to avoid edge artefacts.

Each cell in the network layer can receive a maximum number of afferent synapses (32 in our simulations). Whilst we acknowledge arguments for the utility of inhibitory lateral connections in building functional architecture [8] we simplified our model using the finding [4] that a topographic projection could form in the absence of long-range lateral inhibition. Thus, two excitatory projections are used, a feed-forward and a lateral projection; these projections compete for the synaptic capacity of the network neurons. We assume that an unspecified activity-independent process is capable of guiding the formation of new synapses so that they are distributed around their ideal locations. We assume a Gaussian distribution, since a process which is initially directed towards a target site and then randomly branches on its way would yield a Gaussian distribution of terminations around the target site.

To implement this, where a network cell has less than its maximum number of synapses, the remaining slots are considered "potential synapses". At a fixed "rewiring" rate a synapse from the neurons of the network layer is randomly chosen. If it is a potential synapse a possible pre-synaptic cell is randomly selected and synapse formation occurs when:

$$r < p_{form}.e^{-\frac{\delta^2}{2{\sigma_{form}}^2}} \tag{1}$$

where r is a random number uniformly distributed in the range $(0, 1)$, p_{form} is the peak formation probability, δ is the distance of the possible pre-synaptic cell

from the ideal location of the post-synaptic cell and ${\sigma_{form}}^2$ is the variance of the connection field. In other words a synapse is formed when a uniform random number falls within the area defined by a Gaussian function of distance, scaled according to the peak probability of synapse formation, (which occurs at $\delta = 0$). This is essentially a rejection sampling process.

Lateral connections are formed by the same means as feed-forward connections though σ_{form} is different for each projection and p_{form} is set correspondingly to allow the same overall probability of formation for each projection. In the absence of a general rule for the relative numbers of feed-forward vs lateral connections formed, starting with equal numbers of each is a good basis for observing the relative development of these projections; $\sigma_{form-feedforward}$ is given a larger value than $\sigma_{form-lateral}$, in line with generic parameters given in [8].

If the selected synapse already exists it is considered for elimination. In general we propose that the probability of elimination should be some monotonically decreasing function of weight. Due to the nature of the learning rule we have chosen (STDP; see below in this section), which tends to deliver a bimodal weight distribution, we have simplified probability of elimination to one of 2 values with a higher value for synapses with weights below a certain threshold ($p_{elim-dep}$) and vice versa ($p_{elim-pot}$). Data is scarce on appropriate values for these probabilities, however dendritic spines have been imaged extending and retracting over periods of hours compared with others stable over a month or more [15]. We have used much higher rates so that synapses have several chances to rewire during the short periods for which it was tractable to run simulations, while maintaining a large difference between these probabilities (in fact we used a factor of 180 representing the difference between 4 hours and 1 month).

The rest of our model is strongly based on [4]. We use integrate and fire neurons, where the membrane potential V_{mem} is described by:

$$\tau_{mem}\frac{\delta V_{mem}}{\delta t} = V_{rest} - V_{mem} + g_{ex}(t)(E_{ex} - V_{mem}) \tag{2}$$

where E_{ex} is the excitatory reversal potential, V_{rest} is the resting potential and τ_{mem} is the membrane time constant. Upon reaching a threshold V_{thr}, a spike occurs and V_{mem} is reset to V_{rest}. A presynaptic spike at time 0 causes a synaptic conductance $g_{ex}(t) = ge^{\frac{-t}{\tau_{ex}}}$ (where τ_{ex} is the synaptic time constant); this is cumulative for all presynaptic spikes. Spike-timing-dependent plasticity is implemented such that a presynaptic spike at time t_{pre} and a post-synaptic spike at time t_{post} modify the corresponding synaptic conductance by $g \rightarrow g + g_{max}F(\Delta t)$, where $\Delta t = t_{pre} - t_{post}$ and:

$$F(\Delta t) = \left\{ \begin{array}{l} A_+.e^{(\frac{\Delta t}{\tau_+})}, \quad if \Delta t < 0 \\ -A_-.e^{(\frac{-\Delta t}{\tau_-})}, if \Delta t \geq 0 \end{array} \right\} \tag{3}$$

where $A_{+/-}$ are magnitudes and $\tau_{+/-}$ are time constants for potentiation and depression respectively. This is cumulative for all pre- and post-synaptic spike pairs. g is bounded in the range $0 \leq g \leq g_{max}$.

Parameters were set starting from parameters given in [4]. A+ was increased 20-fold as a concession to limited computational resources for simulations (this should not qualitatively change the model since many plasticity events are still needed to potentiate a depressed synapse). Then key parameters were changed; namely g_{max} (the peak synaptic conductivity), $\tau-/\tau+$ (the ratio of time constants for depression and potentiation) and B (the ratio of potentiation to depression, i.e. A_+/A_-) were changed to maintain key conditions, being: the total weight should be approximately 50% of the maximum possible; the average network neuron firing rate should approximately match the average input firing rate; and the total weight of lateral synapses should roughly match the weight of feed-forward ones. In the interests of simplicity we did not allow for different values of B for different projections feedforward vs recurrent). An unjustified simplification is that new synapses start strong and then get weakened; the opposite case seems more likely. We have used this for simplicity because it avoids the need for any homeostatic mechanisms to kick-start the network.

Each input cell was an independent Poisson process. A stimulus location was chosen and mean firing rates were given a Gaussian distribution around that location based on a peak rate f_{peak} and variance ${\sigma_{stim}}^2$ which was added to a base rate f_{base}. The stimulus location changed regularly every 0.02s. This regularity is a move away from biologically realistic inputs (c.f. [4]); this was a necessary concession to provide stronger correlation cues given the smaller number of synapses per neuron. A further concession was the more extreme values of f_{base} and f_{peak}. σ_{stim} was chosen to be between the values of $\sigma_{form-feedforward}$ and $\sigma_{form-lateral}$ and f_{peak} was set so as to keep the overall mean firing rate at a mean value f_{mean} which gave sufficient difference between f_{base} and f_{peak}.

3 Results

Simulations were run with a C++ function, with initial conditions created and data analysis carried out with Matlab. Simulations used a time step of 0.1ms. Parameters are given in table 1. The mean frequency of rewiring opportunities per potential synapse was 1.22Hz (depressed synapses were therefore eliminated after an average of 33s). Initial placement of synapses was performed by iteratively generating a random pre-synaptic partner and carrying out the test for formation described in section 2. Initially feed-forward and lateral connections were placed separately, each up to their initial number of 16 synapses. Weights were initially maximised. Runs were for 5 minutes of simulated time.

For calculating the preferred location for each target cell, the use of the "centre of mass" measure as in [6] would be erroneous because the space is toroidal and therefore the calculation of preferred location would be skewed by the choice of reference point from which synapses' coordinates are measured. In [6] the reference point for calculating centre of mass of the dendritic synapses of a target cell was chosen as the predefined ideal location, therefore the measures of distance of preferred location were skewed towards the ideal locations dictated by the model. We avoided this by the novel method of searching for the location

Table 1. Simulation parameters

for STDP	for rewiring	for inputs
$g_{max} = 0.2$	$\sigma_{form-feedforward} = 2.5$	$f_{mean} = 20Hz$
$\tau_m = 0.02s$	$\sigma_{form-lateral} = 1$	$f_{base} = 5Hz$
$\tau_+ = 0.02s$	$p_{form-lateral} = 1$	$f_{peak} = 152.8Hz$
$\tau_- = 0.064s$	$p_{form-feedforward} = 0.16$	$\sigma_{stim} = 2$
$A_+ = 0.1s$	$p_{elim-dep} = 0.0245 (= 0.5 * \text{mean formation rate})$	
$B = 1.2$	$p_{elim-pot} = p_{elim-dep}/180 = 1.36 * 10 - 4$	

around which the afferent synapses have the lowest "weighted variance" ($\sigma_{aff}{}^2$), i.e.:

$$\sigma_{aff}^2 = \underset{\boldsymbol{x}}{\operatorname{argmin}} \frac{\sum_i w_i . |\boldsymbol{p}_{xi}|^2}{\sum_i w_i} \tag{4}$$

where i is a sum over synapses, $\boldsymbol{x}$ is a candidate preferred location, $|\boldsymbol{p}_{xi}|$ is the minimum distance from that location of the afferent for synapse i and wi is the weight of the synapse (if connectivity is evaluated without reference to weights, synapses have unitary weight). We implemented this with an iterative search over each whole number location in each dimension and then a further iteration to locate the preferred location to 1/10th of a unit of distance (the unit is the distance between two adjacent neurons). Note that in the non-toroidal case this measure is equivalent to the centre of mass, as used in [3].

Having calculated the preferred location for all the neurons in the network layer we took the mean of the distance of this preferred location from the ideal location to give an Average Absolute Deviation (AAD) for the projection. By reporting both AAD and mean σ_{aff} for a projection we have a basis for separating its variance from the deviation of its preferred location from its ideal location. However AAD and mean σ_{aff} are both dependent on the numbers and strengths of synapses and these can change during development. Therefore to observe the effect of the activity-dependent development mechanism irrespective of changes in synapse number and strength we made comparison in two ways. Firstly, for evaluating change in mapping quality based only on changes in connectivity without considering the weights of synapses we created a new map taking the final number of synapses for each network neuron and randomly placing them in the same way as the initial synapses were placed. We then calculated σ_{aff} and AD for each neuron in each of the maps and compared the averages of these (i.e. mean σ_{aff} and AAD), applying significance tests between the values of two populations of neurons, i.e. all the neurons on the final map vs all those on the reconstructed map. Having established what effect there was on connectivity we considered the additional contribution of weight changes by creating a new map with the same topology, taking the final weights of synapses for each network neuron and randomly reassigning these weights amongst the

existing synapses for that neuron. We then compared the two maps as described above.

Three main experiments were carried out: Case 1 had both rewiring and input correlations, as described in section 2; case 2 had input correlations but no rewiring; case 3 had rewiring but no input correlations (i.e. all input neurons fired at fmean). The results are given in table 2. For comparisons, mean σ_{aff}

Table 2. Summary of simulation results: Case 1: Rewiring and input correlations; Case 2: Input correlations and no rewiring; Case 3: Rewiring and no input correlations

Case	**1**	**2**	**3**
Network neuron mean spike rate	24.7	17.4	10.5
Final mean no. feed-forward incoming synapses per network neuron	14.1	NA	12.5
Weight as proportion of max for the initial no. of synapses	0.60	0.36	0.33
Mean $\sigma_{aff-init}$	2.36	2.36	2.36
Mean $\sigma_{aff-final-con-shuffled}$	2.34	NA	2.28
Mean $\sigma_{aff-final-con}$	1.95	2.36	2.17
Mean $\sigma_{aff-final-weight-shuffled}$	1.97	2.16	2.04
Mean $\sigma_{aff-final-weight}$	1.70	1.98	1.95
AAD_{init}	0.78	0.78	0.78
$AAD_{final-con-shuffled}$	0.90	NA	0.96
$AAD_{final-con}$	0.83	0.78	0.93
$AAD_{final-weight-shuffled}$	0.96	1.40	1.33
$AAD_{final-weight}$	0.95	1.58	1.34

and AAD were each calculated for the feed-forward connections of the following networks: The initial state with weights not considered (recall that all weights were initially maximised) these results are suffixed *init*, i.e. AAD_{init}; the final network with weights not considered but only connectivity with all synapses weighted equally, i.e. $AAD_{final-con}$; for comparison with $AAD_{final-con}$, the final number of synapses for each network neuron randomly placed in the same way as the initial synapses (not applicable for simulations with no rewiring), i.e. $AAD_{final-con-shuffled}$; the final network including weights, i.e. $AAD_{final-weight}$; for comparison with $AAD_{final-weight}$, the final connectivity for each network neuron with the actual weights of the final synapses for each network neuron randomly reassigned amongst the existing synapses, i.e. $AAD_{final-weight-shuffled}$. Results were compared using Kolmogorov-Smirnov (KS) tests on AD and σ_{aff} for incoming connections for each network neuron over the whole network layer for a single simulation of each of the two conditions under consideration.

4 Discussion

We observe the effect of rewiring by comparing case 1 (with rewiring) and case 2 (without rewiring). Considering topology change, in case 1 mean $\sigma_{aff-final-con}$

drops to 1.95, c.f. 2.34 for mean $\sigma_{aff-final-con-shuffled}$; this drop is significant (KS, p=5.3e-25). In case 2 mean $\sigma_{aff-final-con}$ is constrained to remain at mean $\sigma_{aff-init} = 2.36$. Considering weight change, in case 1 mean $\sigma_{aff-final-weight}$ drops to 1.70, c.f. 1.97 for mean $\sigma_{aff-final-weight-shuffled}$. In case 2, mean $\sigma_{aff-fin-weight}$ drops to 1.98, c.f. 2.16 for mean $\sigma_{aff-final-weight-shuffled}$. Both drops are significant (KS, p=3.6e-09 and 0.0024 respectively).

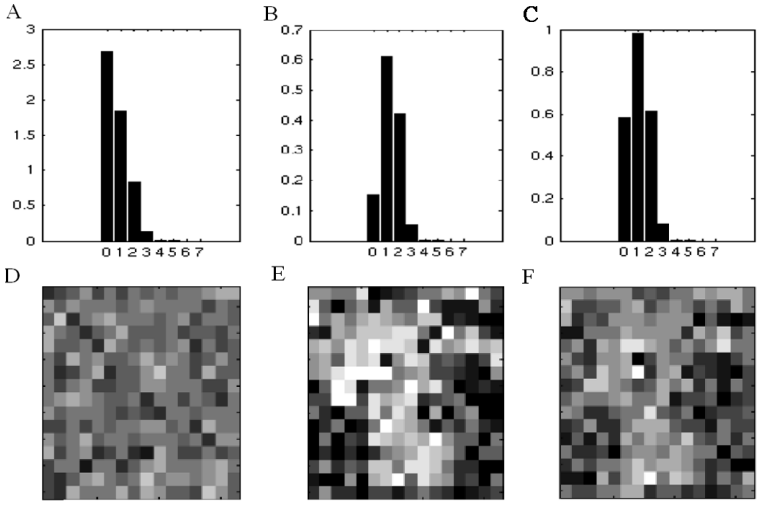

Fig. 1. A-C: Normalised weight density of incoming lateral synapses (weight/unit area; y-axis) radially sampled and interpolated at given distances of pre-synaptic neuron from post-synaptic neuron (x-axis), averaged across population. D-F: ocular preference, i.e. preference for cells from the two intra-correlated input spaces interspersed in the input space, for each network cell on a scale from white to black. A,D: initial. B,E: final, considering synaptic weights. C,F: final, all synapses with unitary weight.

Mean $\sigma_{aff-final-weight}$ appears to be lower in case 1 than case 2. We cannot say for sure that this superior reduction of variance is due to the effect of the rewiring mechanism because the different numbers of final synapses in each case make a comparison impossible, however there is a good reason to believe that this is so: the drop in mean $\sigma_{aff-final-con}$. This drop on its own indicates that the rewiring mechanism has helped to reduce variance and would also lay the groundwork for different final measures of σ_{aff} when weights are considered.

We can also see qualitatively that the effect of rewiring is to embed in the connectivity of the network input preferences which arise through the weight changes mediated by the learning rule. STDP favours causal inputs with the lowest latency and local excitatory lateral connections tend to lose the competition with excitatory feed-forward connections as they have a higher latency [4]. The extreme of this effect can be seen in synapses from a network neuron

back to itself (recurrent synapses). The placement rule allows these synapses to form, however these synapses only ever receive a pre-synaptic spike immediately following a post-synaptic spike and therefore they are always depressed by the learning rule. Figure 1A shows the initial density of incoming lateral synapses from pre-synaptic partners at given distances out from the post-synaptic neuron. It can be seen that the average neuron receives more synapses from itself (those at x-position 0) than from any of its closest neighbours. Figure 1B shows the final distribution where synapses are weighted. The recurrent synapses have been depressed much more than their neighbours. Figure 1C shows the final distribution only considering numbers of synapses and not their weights. The proportion of recurrent synapses to lateral synapses with neighbours has reduced from the initial state, due to the preferential elimination of the weak recurrent synapses.

As a further demonstration of the effect of rewiring a simulation was carried out with the input neurons divided into two groups, mimicking the effect of binocular inputs. The groups were interspersed in a regular diagonal pattern, i.e. each input neuron is in the opposite group to its 4 adjacent neurons; the stimulus location switched between the two groups every time it changed. To keep the overall input rate the same the peak firing rate was doubled. Figure 1D shows the initial preference of each network neuron for input neurons in the two groups. Figure 1E shows the final ocular dominance map where synapses are weighted. Although the space used was too small and the result of the learning rule with a small number of synapses too random for familiar striped ocular dominance patterns to emerge (c.f. [3]) ocular dominance zones can be seen. This pattern is reflected in the final map of connectivity in Figure 1F, where synaptic weights are not considered; another example of weight patterns caused by input activity becoming embedded in connectivity patterns.

Considering the effect of the algorithm on AAD, in case 2 $AAD_{final-weight}$ is significantly increased c.f. $AAD_{final-weight-shuffled}$ (KS, p=0.0084). In case 1 the corresponding change is not significant (KS, p=0.94). In case 1 the drop in $AAD_{final-con}$ c.f. $AAD_{final-con-shuffled}$ is not significant (KS, p=0.16).

The basic action of weight-independent STDP on a set of incoming synapses for a single neuron is to deliver a bimodal weight distribution [4]. Where there are input correlations these cause the more correlated inputs to be maximised and the less- or un-correlated inputs to be minimised. The effect of both the input correlations and the local excitatory lateral synapses on each individual incoming connection field then should be to cause a patch of neighbouring synapses to become potentiated and for outliers from this patch to be depressed. The location of the patch will be random; it is likely to form near the ideal location because there should be a denser concentration of synapses there, however the centre of the patch is unlikely to fall exactly on the ideal location but rather a certain mean distance from it. This introduces a shift of preferred location from the ideal location. Rewiring cannot be expected to eliminate this error but it might be expected to allow the patch to move towards the centre as σ_{aff} reduces due to the preferential placement of synapses towards the centre. However in our simulations AAD did not improve. The slight drop in $AAD_{final-con}$ c.f.

$AAD_{final-con-shuffled}$ is not significant but in any case a drop in AAD could only be a result of the reduction in mean σ_{aff} because $AAD_{final-weight}$ does not decrease, rather it stays the same (as in case 1) or increases (as in case 2). That is to say, the result of the weight changes is not to drive the preferred location towards the ideal. Rather, the improvement of topography is driven by the continued placement of synapses towards the ideal location; the activity-dependent mechanism simply facilitates by allowing the incoming connection field to be narrowed by the preferential elimination of outliers.

Considering the role of input correlations, in case 3 (rewiring but no input correlations) mean $\sigma_{aff-final-con} = 2.17$, vs 2.28 for mean $\sigma_{aff-final-con-shuffled}$; this is significant (KS, p=0.011). Mean $\sigma_{aff-final-weight} = 1.95$ vs 2.04 for mean $\sigma_{aff-final-weight-shuffled}$; this is not significant (KS, p=0.16).

Although the slight drop in mean $\sigma_{aff-final-weight}$ is not statistically significant, it is nevertheless a sufficient cue to drive the narrowing of the incoming connection fields, as evidenced by the drop in mean $\sigma_{aff-final-con}$. It was shown [8] that functional architecture could form in the absence of any input except uncorrelated random noise. We show that this applies to topographic map refinement as well, although our explanation differs: A spike from a single input neuron will excite a given network neuron and any other of its neighbours which have a feed-forward synapse from that input. Thus the neuron will also on average receive some excitation from lateral connections because of that spike. Because network neurons sample afferent neurons more densely around their ideal locations they are more likely to share an afferent with a neighbour if that afferent is close to their ideal location. Thus synapses from afferents closer to the ideal location are more likely to be potentiated. Therefore the gradient of connection density set up by the activity-independent placement process acts as a cue which allows the preferential elimination of outliers, giving a reduction in variance as described above in this section.

5 Conclusions

We have presented a model of topographic development including both weight and wiring plasticity, which follows the reasonable assumptions that synapses preferentially form in locations to which their axons are guided and that weaker synapses are more likely to be eliminated. We have shown that spatially correlated inputs help to create patterns of synaptic weights which favour narrower projections, but the spatial correlations are not necessary for some reduction of variance to occur (extending a result from [8]). A weight-change mechanism and a rewiring mechanism can work together to achieve a greater effect than the weight changes alone, with the rewiring mechanism acting to embed patterns of synaptic strengths in the network topology; this is as one would expect, though it has not been demonstrated quantitatively before, to our knowledge. The accuracy of preferred locations for network neurons however may not necessarily improve when synapses are formed based on distributions with on-average perfect topography to start with. The novel division of mapping quality into the

quantities of mean σ_{aff} and AAD is therefore a useful means for investigating these effects, and we have demonstrated a method of applying statistical significance tests to extract highly significant effects from small-scale simulations.

Acknowledgements

We are grateful to Guy Billings for providing the basis of the simulator code. This work was funded by EPSRC.

References

1. Willshaw, D., von der Malsburg, C.: How patterned neural connections can be set up by self-organisation. Proc. R. Soc. Lond. B. **194** (1976) 431–445
2. Miller, K., Keller, J., Stryker, M.: Ocular dominance column development: analysis and simulation. Science **245** (1989) 605 615
3. Goodhill, G.: Topography and ocular dominance: a model exploring positive correlations. Biological Cybernetics **69** (1993) 109–118
4. Song, S., Abbott, L.: Cortical development and remapping through spike timing-dependent plasticity. Neuron **32** (Oct 2001) 339–350
5. Willshaw, D.: Analysis of mouse Epha knockins and knockouts suggests that retinal axons reprogramme target cells to form ordered retinotopic maps. Development **133** (2006) 2705–2717
6. Elliott, T., Shadbolt, N.: A neurotrophic model of the development of the retinogeniculocortical pathway induced by spontaneous retinal waves. Journal of Neuroscience **19** (1999) 7951–7970
7. Miller, K.: Equivalence of a sprouting-and-retraction model and correlation-based plasticity models of neural development. Neural Computation **10** (1998) 529–547
8. Miikkulainen, R., Bednar, J., Choe, Y., Sirosh, J.: Computational Maps in the Visual Cortex. Springer, New York (2005)
9. Willshaw, D., von der Malsburg, C.: A marker induction mechanism for the establishment of ordered neural mappings: its application to the retinotectal problem. Philosophical Transactions of the Royal Society of London. Series B, Biological Sciences **287** (1979) 203–243
10. Bamford, S., Murray, A., Willshaw, D.: Large developing axonal arbors using a distributed and locally-reprogrammable address-event receiver. International Joint Conference on Neural Networks (IJCNN) (2008)
11. Sperry, R.: Chemoaffinity in the orderly growth of nerve fiber patterns and connections. Proc. Natl. Acad. Sci. USA **50** (1963) 703–709
12. Ruthazer, E., Cline, H.: Insights into activity-dependent map formation from the retinotectal system: A middle-of-the-brain perspective. Journal of Neurobiology **59** (2004) 134–146
13. Frean, M.: A model for adjustment of the retinotectal mapping, based on eph-dependent regulation of ephrin levels. In: Fifteenth Annual Computational Neuroscience Meeting, Edinburgh. (2006)
14. Swindale, N.: The development of topography in the visual cortex: a review of models. Network: Computation in Neural Systems **7** (1996) 161–247
15. Grutzendler, J., Kasthuri, N., Gan, W.: Long-term dendritic spine stability in the adult cortex. Nature **420** (2002) 812–816